9-1996

Post-collision Interactions in the Auger Decay of the Ar L-shell

James A.R. Samson
Behlen Laboratory of Physics

Wayne C. Stolte
University of Nevada, Las Vegas, wcstolte@lbl.gov

Z. X. He
IBM, Inc.

J. N. Cutler
Wright Patterson AFB

D. Hansen
University of Nevada, Las Vegas

Postcollision interactions in the Auger decay of the Ar L shell

James A. R. Samson, W. C. Stolte, Z. X. He,* J. N. Cutler,† and D. Hansen‡
Behlen Laboratory of Physics, University of Nebraska, Lincoln, Nebraska 68588-0111
(Received 16 January 1996; revised manuscript received 4 April 1996)

The photoionization cross sections for Ar^+ through Ar^{4+}, produced by the Auger decay of a $2p$ hole in argon, have been measured between 242 eV and 253 eV by the use of synchrotron radiation. The high resolution of the monochromator has allowed a detailed study of the postcollision interactions that occur in this spectral region. The concept of photoelectron recapture by Ar^{2+} to produce the Ar^+ continuum is studied. The relative values of the quantum-mechanical calculations of the photoelectron recapture probability are shown to be in excellent agreement with the present data. The magnitude and shape of the Ar^{2+} continuum has been explained on the basis that about 67% of the recaptured photoelectrons produce excited states of Ar^+ which subsequently reemit the electrons by autoionization. [S1050-2947(96)02308-6]

PACS number(s): 32.80.Hd, 32.80.Dz, 32.80.Fb

I. INTRODUCTION

There has been considerable interest recently in the phenomenon of postcollision interactions (PCI) [1–39]. This process was first studied by Barker and Berry [1] in 1966 with experiments involving autoionizing states produced by ion-atom collisions. They observed an energy shift and broadening in their electron energy spectra. This was explained as an interaction between electrons, produced in the decay of the autoionized states, and the field of the slow receding ion. In similar studies (but with electron-atom collisions) Hicks *et al.* [2] referred to this model as a postcollision interaction. Numerous experiments have been performed since then [3–27] and semiclassical and quantum-mechanical theories have appeared which successfully explain the shifts and broadening of the fast ejected electrons [28–39].

In the present work we are interested in near threshold photoionization experiments involving postcollision effects related to the Auger decay of a vacancy in the Ar L shell. The semiclassical description of the PCI effect can be described briefly as follows:

When an inner-shell electron is photoionized just above its ionization threshold a slow photoelectron is produced receding away from the singly ionized core. Subsequent decay of the vacancy by an Auger process produces a fast Auger electron. If the lifetime of the inner-shell vacancy is sufficiently short the fast Auger electron can overtake the photoelectron, which is then exposed to a doubly charged ion core. The photoelectron will be retarded losing a certain amount of energy, whereas the Auger electron (now exposed to a singly charged core) gains energy. This exchange of energy results in a distorted line shape and a shift in the peak energy of both electrons. In fact, even below the ionization threshold the short lifetime of the Auger decay ($\sim 10^{-15}$ s) allows the Auger electron to interact with the primary excited photoelectron. This interaction determines the final n-level location of the photoelectron and causes distortion in the energy profile of the Auger electron. Such distortions have been reported by de Gouw *et al.* [24,25] for as much as 0.6 eV below threshold.

Much of the work in this area has concentrated on measurements of the Auger-electron energies, their line profiles, and peak energy shifts. These results are all well described by the semiclassical models of Niehaus [31], Russek and Mehlhorn [32], and by van der Straten, Morgenstern, and Niehaus [33].

Another consequence of PCI is its effect on the production of the various stages of ionization in the Auger decay process. If we consider the case of a vacancy in the Ar $L_{2,3}$ shell (where the probability of decay by fluorescence is very much smaller than that by an Auger decay [40,41]) we would expect the lowest stage of ionization to be Ar^{2+}. This is, in fact, what is observed when photoionization occurs well above the $2p$ ionization threshold. However, near threshold it has long been predicted that the energy lost by the photoelectron would be recaptured causing singly charged ions to be produced, presumably, in highly excited states [29–32,35]. Van der Wiel, Wight, and Tol [7] provided the first experimental evidence that Ar^+ ions were formed in the Auger decay. They used an electron energy loss scattering experiment and noted that the sum of the Ar^{2+} and Ar^{3+} yields divided by the total energy-loss signal increased for the first few eV above threshold before remaining constant. They interpreted this variation as being caused by the conversion of Ar^{2+} to Ar^+ by electron capture. Direct measurements of Ar^+ ions produced above threshold have now been measured by several groups [15,21,23]. The electron recapture probability curve has been calculated by Eberhardt *et al.* [21] using the semiclassical model of Russek and Mehlorn [32] and applied above the L_2 edge. The exponential type of decrease in the Ar^+ signal as a function of the excess energy of the photoelectron above the L_2 edge is in good agreement with their experimental results. The recent quantum-mechanical calculations of Tulkki *et al.* [35] appear to give a better fit to the experimental data.

In the present work we expand in more detail on our

*Present address: IBM, Inc., Burlington, VT 05452.
†Present address: Dept. of Chemistry, University of Western Ontario, London, Ontario, Canada N6A 5B7.
‡Present address: Department of Chemistry, University of Nevada, Las Vegas, NV 89154.

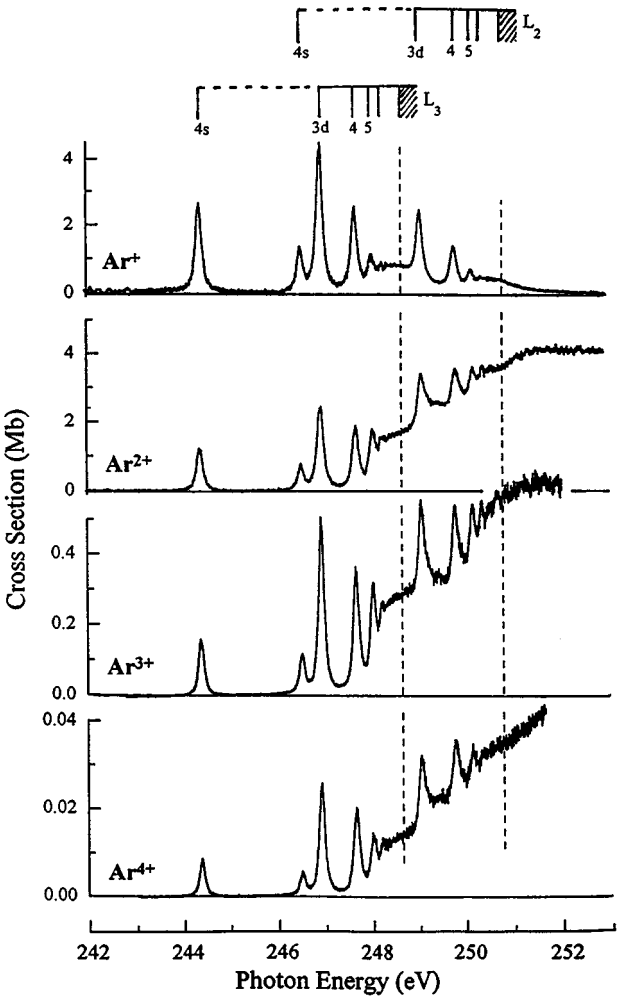

FIG. 1. Photoionization cross sections of Ar^+ through Ar^{4+} produced by the decay of a $2p$ hole in argon. The resonance lines represent the transitions $2p^{-1}(3s^2 3p^6)nd$, $(n+1)s$, where $n \geqslant 3$. The instrumental resolution was 80 meV for the Ar^+ and Ar^{2+} spectra and 54 meV for Ar^{3+} and Ar^{4+}.

recently reported studies of multiple ionization [42–44]. We have measured the Ar ion yields from Ar^+ through Ar^{4+} at photon energies between 242 and 253 eV, but with much higher resolution (20–60 meV) than previous studies. The effects of electron recapture can clearly be seen in the Ar^+ spectrum above the L_2 and L_3 edges. In addition, the Ar^{2+} yield does not drop immediately to zero at the $L_{2,3}$ thresholds as would be expected if the recapture probability was 100% at threshold. This observation has not been noted before, neither in experimental nor theoretical studies. We will present data and analysis that explains this anomaly as a consequence of electron recapture into autoionizing states with subsequent reemission of the electron as the state deexcites.

II. EXPERIMENT

Measurements of the ion yields produced by Auger decay of the argon $2p^{-1}$ vacancy were performed at the Lawrence Berkeley National Laboratory's Advanced Light Source (ALS). Two different beamlines were utilized. The 8 cm undulator beamline 9.0.1 provided the highest resolution and photon flux in the 250 eV energy range. The photon flux was typically 5×10^{12} photons/s. With monochromator slits of 35×45 μm the resolution obtained was about 40 meV, full width at half maximum (FWHM) at 240 eV in the first-order spectrum. For line width measurements we were able to utilize the second-order spectrum (at 120 eV), obtaining 20 meV resolution. Measurements were also made on the 6.3.2 bending magnet beamline. Although the photon flux and resolution were lower ($\sim$80 meV energy resolution at 250 eV) this beamline was free from spurious noise associated with the undulators. Calibration of the monochromator energy scale was achieved by using the Ar $4s$ resonance line at 244.39 eV $\pm$0.01 eV determined by King and Read [45].

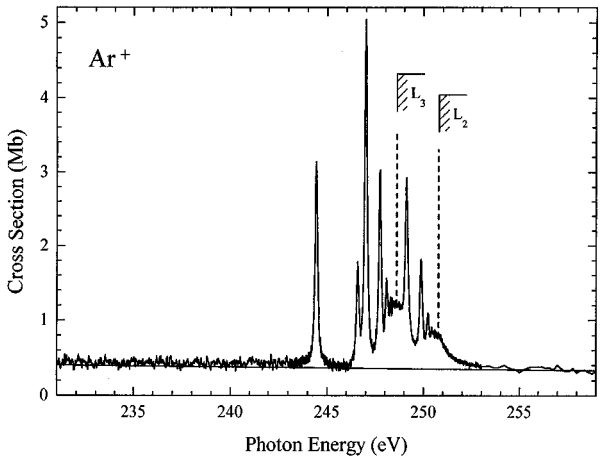

FIG. 2. Photoionization cross section for producing Ar^+ by ejection of a $2p$ electron. The slowly decreasing background continuum is caused by photoionization of a valence shell electron.

A magnetic mass spectrometer was used to identify the various degrees of ionization produced with photon energy scans covering the range 242 to 253 eV. Data were taken in 2 to 20 meV steps. A time-of-flight mass spectrometer was used to determine the branching ratios of Ar^+ through Ar^{4+} at the L_3 threshold.

III. RESULTS AND DISCUSSION

A. Ion yields: Estimate of absolute cross sections

The ion yield spectra for Ar^+ through Ar^{4+} are shown in Fig. 1. All scans were divided by the incident photon detector signal and were independent of each other. The detector (an aluminum photodiode) had an efficiency that essentially remained constant over the energy range studied. Thus each scan represents a relative cross section. To relate these scans to one another and place them on an absolute scale the following procedure was followed:

The relative yields, or branching ratios, for each stage of ionization were measured at the L_3 edge (248.63 eV) by use of a time-of-flight (TOF) mass spectrometer. The actual counts for Ar^+ and Ar^{2+} were corrected by subtracting the background counts produced by direct photoionization of the argon valence shell. This was determined from ion yield spectra obtained using the magnetic mass spectrometer. A typical spectrum of Ar^+ is shown in Fig. 2. This shows the

Ar^+ signal produced by photoionization of the Ar $L_{2,3}$ shell superimposed on a slowly decreasing continuum caused by direct photoionization of the argon valence shell. The background constituted 30% of the Ar^+ signal at the L_3 edge. A similar set of data were taken for Ar^{2+}. In this case a background of only 5% was observed at the L_3 edge. No appreciable background was observed for Ar^{3+} and Ar^{4+}.

The relative yields were then converted into absolute values by multiplying their values at the L_3 edge by the total L_3 cross section, namely, 2.80 Mb$\pm$5%. This value was obtained from our analysis of the data of Watson [46], Denne [47], and Gilberg, Hanus, and Foltz [48]. The resulting absolute cross sections for the production of Ar^+ through Ar^{4+} at the L_3 edge are, respectively, 0.82, 1.69, 0.28, and 0.014 Mb. The cross section scales in Fig. 1 are based on these values. Thus from Fig. 1 the partial cross sections at the L_2 edge for Ar^+ through Ar^{4+} are, respectively, 0.43, 3.58, 0.56, and 0.035 Mb, which yields a total cross section of 4.6 Mb. From our above analysis of the literature data we estimate that the total cross section at the L_2 edge should be 4.2 Mb, which is in keeping with the expected ratio of two between the L_3 and L_2 cross sections. This indicates an overall uncertainty in the present results of about 10%.

B. Photoelectron recapture probability: Ar^+ production

In a normal Auger decay process a photoelectron and an Auger electron are ejected producing Ar^{2+}. Therefore, the probability that a photoelectron will be recaptured must equal the probability that Ar^+ will be created (excluding valence shell photoionization).

Tulkki *et al.* [35] have made a quantum-mechanical calculation of the recapture probability $P(E_{ex})$ as a function of the excess energy E_{ex} above the L_2 threshold using a value of $\Gamma=0.126$ eV for the half-width of the $2p^{-1}$ inner-shell energy level. Their tabulated values of $P(E_{ex})$ are expressed as a percentage based on $P(E_{ex}=0)=100\%$ at threshold and cover the range $E_{ex}=0.25$ eV to 2.5 eV. Numerical difficulties prevented the determination of $P(E_{ex})$ for values of E_{ex} less than 0.25 eV.[1] They have provided an approximate equation for the recapture probability curve to extend their results to higher energies and to illustrate the dependence of P on E_{ex} and Γ, namely,

$$P(E_{ex}) \simeq 1-\exp(-\Gamma/E_{ex}). \quad (1)$$

Their more rigorous calculation provides a broader curve that merges into the form of Eq. (1) at higher values of E_{ex} (greater than about 4.5 eV). Tulkki *et al.* note that the dependence of the recapture probability on E_{ex}, above either the L_2 or L_3 thresholds should be the same. Thus their tabulated data and results from Eq. (1) can be used for either continua. We have converted these values into cross sections, measured in Mb units, by equating $P(E_{ex}=0)=1$ to 0.82 Mb at the L_3 threshold and to 0.43 Mb at the L_2 threshold. These results are shown in Figs. 3 and 4 by the dashed lines.

To determine the experimental electron recapture probability curve we note that the data above the L_2 edge represents the sum of the L_2 probability curve sitting on top of the L_3 continuum tail. Thus we first subtract the theoretical L_3 continuum from the experimental (L_2+L_3) continuum to obtain an approximate probability curve. We then take this curve and normalize it to the L_3 threshold. This procedure provides a new L_3 continuum base line. Subtracting this new base line from our experimental (L_2+L_3) continuum gives a revised probability curve. Renormalization of the revised curve at the L_3 threshold does not change appreciably the magnitude of our new base line. Thus we have extracted a semiexperimental recapture probability curve. The results are given in Table I and displayed in Fig. 3 and Fig. 4 (solid line curve). The accuracy of the data beyond 2.5 eV above the L_2 threshold depends on the accuracy of Eq. (1). The theoretical and experimental curves above the L_2 threshold have nearly identical shapes between $E_{ex}=0.25$ eV and 2.5 eV,

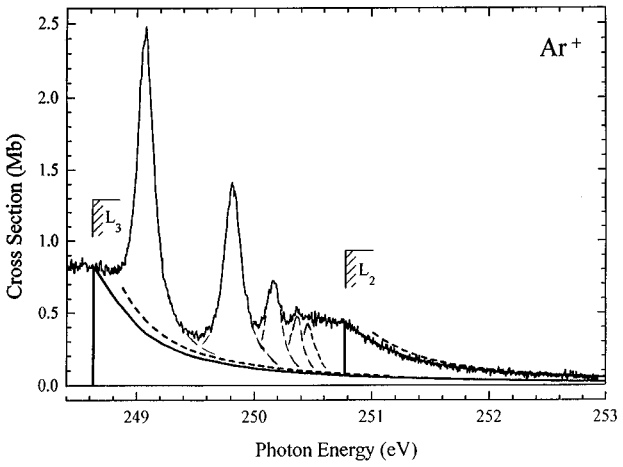

FIG. 3. The Ar^+ ionization continuum produced by postcollision interactions between the Auger electron and the photoelectron causing recapture of the photoelectron. The dashed line represents calculated recapture probability [35]. The solid line curve represents the semiexperimental recapture probability based on the data above the L_2 threshold.

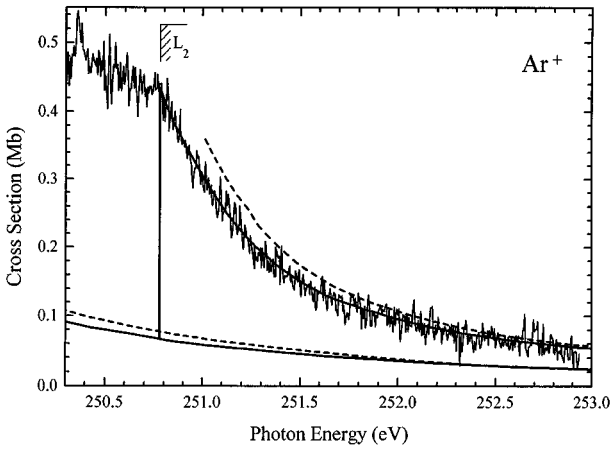

FIG. 4. Ar^+ ionization cross section in the vicinity of the L_2 threshold. The experimental L_2 continuum is shown sitting on the tail of the L_3 continuum (solid line). The dashed lines represent the calculated results [35].

[1]T. Åberg (private communication).

TABLE I. Photoelectron recapture probability P as a function of the excess energy E_{ex} above the Ar $L_{2,3}$ thresholds.

E_{ex} (eV)	P(%)	E_{ex} (eV)	P(%)	E_{ex} (eV)	P(%)
0	100	1.0	20.5	3.0	5.1
0.1	86.6	1.2	16.5	3.2	4.7
0.2	71.5	1.4	13.6	3.4	4.3
0.3	59.5	1.6	11.7	3.6	3.9
0.4	48.5	1.8	10.1	3.8	3.6
0.5	40.4	2.0	9.0	4.0	3.3
0.6	34.2	2.2	7.8	4.2	3.1
0.7	29.6	2.4	7.0	4.4	2.9
0.8	25.5	2.6	6.3	4.6	2.7
0.9	22.6	2.8	5.7	4.8	2.6

but their absolute magnitudes differ by a constant 22.5% over this range. The Ar^+ continuum decreases immediately at the L_2 threshold, which implies an immediate increase in the production of Ar^{2+}. There is no sign in the Ar^+ continuum of a plateau beyond the threshold that would have indicated a delayed Ar^{2+} onset as observed in the argon K-$L_{2,3}L_{2,3}$ decay by Armen, Levin, and Sellin [39].

C. Electron recapture and reemission: Ar^{2+} production

When the L shell of Ar is photoionized the PCI effect causes the photoelectron to lose energy. The amount of energy lost by the photoelectron decreases as the incident photon energy increases. The loss of energy shows up as an increase in the peak energy and broadening of the Auger electron lines. This effect has been well documented and persists well above the $L_{2,3}$ threshold, certainly for at least 11 eV above threshold [14,24,25]. The importance of this observation is that no *unaffected* Auger line is observed in the threshold region [24,25]. Thus all photoelectrons must lose some energy. Therefore, at threshold *all* ejected photoelectrons must be recaptured. This requires that the Ar^{2+} cross section should drop to zero at the L_3 threshold. As can be seen in Fig. 1 this is not the case. This anomaly can be resolved if the photoelectrons are recaptured into high-lying Rydberg states forming $Ar^{+}*$. A certain fraction of these states will then autoionize back into the Ar^{2+} continuum. This fraction can be determined from the experimental data as follows:

As we have seen, the presence of Ar^+ is a consequence of electron recapture by the Ar^{2+} ion. Therefore, the magnitude of the Ar^+ signal at threshold must equal the amount of Ar^{2+} permanently lost at threshold. We have assumed that there is no appreciable contribution to Ar^{2+} from electron recapture by Ar^{3+}. Adding the Ar^+ and Ar^{2+} cross sections at the L_3 threshold, we see that the Ar^+ signal is 33% of the total sum. That is, only 33% of the electrons that are recaptured remain captured and 67% must be reemitted.

To derive the shape of the Ar^{2+} curve as a function of E_{ex} we note that because the function P represents the probability that Ar^+ will be formed then the function $(1-P)$ represents the probability that Ar^{2+} will be observed. In the absence of any PCI effect (i.e., $P=0$) we can represent the Ar^{2+} ion yield by the rectangle shown in Fig. 5 (dotted lines). When the recapture probability is 100% at threshold $[P(E_{ex}=0)=P_{th}=1]$ we obtain the dashed line curve for Ar^{2+} as a function of E_{ex} by using the data from Table I. The area between the dotted and dashed lines represents the production of Ar^+ caused by electron recapture. However, if electron reemission occurs then the threshold value is less than unity. In the present study $P_{th}=33\%$, which gives the solid line curve in Fig. 5. The shaded area, between the solid and dashed line, must represent the fraction of the captured photoelectrons that are reemitted through autoionization of the high-lying excited states. This fraction is 67% of the total area above the dashed line. That is, 67% of the captured photoelectrons are reemitted at any value of E_{ex}. With this normalization ($P_{th}=33\%$) the plot of $(1-P)$ vs E_{ex} is given by the solid line curve and the total area below that line represents the experimental production of Ar^{2+}. A similar analysis at the L_2 threshold gives a value of about 76%. However, this latter value is less accurate because of the problems in determining the relative cross sections of the overlapping L_2 and L_3 continua.

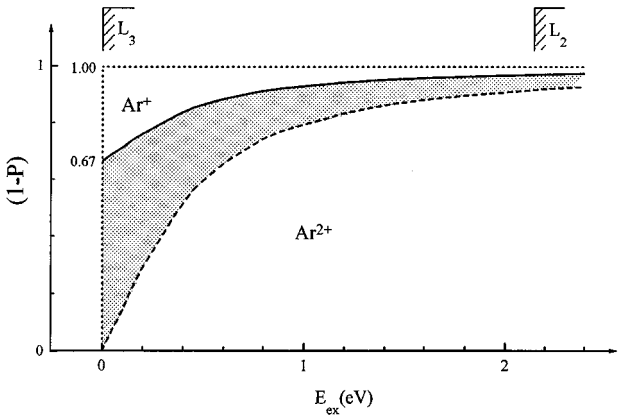

FIG. 5. The curves $(1-P)$ vs E_{ex} represent the different probabilities for producing Ar^{2+} when the threshold values P_{th} vary. $P_{th}=0$ dotted line; $P_{th}=0.33$ solid line; $P_{th}=1$ dashed line.

To compare the shape of the derived Ar^{2+} curve with experiment we take the solid line curve for Ar^{2+} in Fig. 5 and normalize its threshold value to the L_3 experimental cross section for Ar^{2+}. We repeat this procedure, normalizing at the L_2 edge but using the L_3 continuum as a base line. Adding these two curves we compare the results with the Ar^{2+} spectrum in Fig. 6. There is excellent agreement with the shape of the experimental curve.

From the above procedure we can estimate the fraction of the electrons captured by Ar^{3+} and Ar^{4+} that remain captured. Namely, choosing (by trial and error) a value of the P_{th} at the L_3 threshold such that the curve $(1-P)$ vs E_{ex} provides a reasonable continuum base line for the $(2p^{-1})3d$ line in the Ar^{3+} spectrum. We obtain $P_{th}\sim 0.15$ which contributes about 0.04 Mb to the Ar^{2+} production at threshold, an increase of $\sim 2\%$. For the A^{4+} spectrum $P_{th}\sim 0.50$, contributing about 0.01 Mb to the Ar^{3+} production. Thus our earlier assumption to ignore any contribution from Ar^{3+} to Ar^{2+} appears to be justified.

To understand the mechanism and magnitude of the electron reemission we note that the Auger decay of the $2p^{-1}$

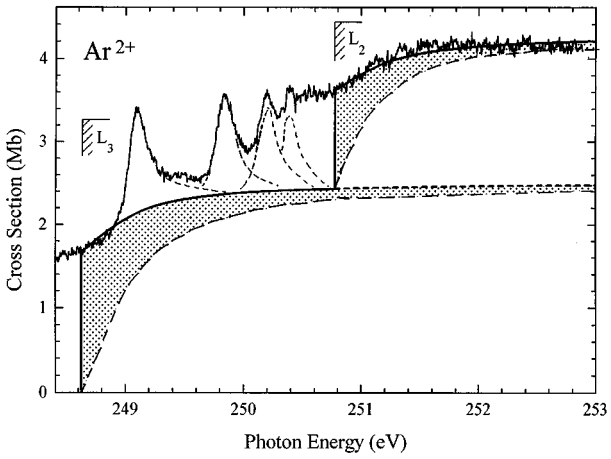

FIG. 6. The Ar^{2+} continuum. The predicted Ar^{2+} yield is given by the probability function $(1-P)$. If electron recapture is 100% at the $L_{2,3}$ thresholds ($P=1$), then the Ar^{2+} yield is represented by the unshaded area under the dashed line. The disagreement with the experiment implies that at threshold 67% of the recaptured electrons must be reemitted. That is, the Ar^{2+} yield must be represented by the curve $(1-P)$ with $P=0.33$ at threshold. This curve is shown by the solid line. The shaded area represents the contribution to Ar^{2+} by electron reemission.

vacancy results in the Ar^{2+} ion being left mainly in any one of six major final states [49,50], namely,

$$Ar^{2+}(3s^2 3p^4)^3P,{}^1D,{}^1S + e_{ph} + e'_A, \tag{2}$$

$$Ar^{2+}(3s3p^5)^3P,{}^1P + e_{ph} + e''_A, \tag{3}$$

$$Ar^{2+}(3s^0 3p^6)^1S + e_{ph} + e'''_A, \tag{4}$$

where e_{ph} represents the primary photoelectron and e_A represents the Auger electron. The energy of the Auger electrons depend on the final state involved as indicated by the primes. The energies of the Auger electrons lie between 170 and 207 eV. Therefore, $E(e_A) \gg E(e_{ph})$ in the vicinity of the $L_{2,3}$ thresholds. We assume electron recapture to be equally probable for each of the above states producing $Ar^{+}*$. If the newly formed $Ar^{+}*$ state decays via autoionization then we have electron reemission producing Ar^{2+}. A radiative decay would produce only Ar^{+}. For example, electron recapture into the ^{3}P state of Eq. (2) gives

$$Ar^{+}*(3s^2 3p^4)^3P n\ell. \tag{5}$$

This state lies below the double ionization threshold and, therefore, can only relax by radiative decay. Thus if we know both the percent distribution for producing the various Ar^{2+} states, given in Eqs. (2)–(4), and the relative probability for radiative vs nonradiative decay of the $Ar^{+}*$ states, created by electron recapture, then we can determine the amount of electron reemission that takes place.

Armen and Larkins [51,52] have recently calculated the rates for radiative and nonradiative decay (autoionization) of the $Ar^{+}(3s3p^5)n\ell$ state. Their results predict that if autoionization decay is energetically possible it will be the dominant decay path. A similar calculation for the $Ar^{+}(3s^2 4p^4)^1D,{}^1Sn\ell$ states showed that these states would decay through a valence-multiplet change to $Ar^{2+}(3s^2 3p^4)^3P + e$, provided the energies of these states lie above the double ionization ground state. They have referred to these transitions as valence-participator-Auger decay and valence-multiplet-Auger decay, respectively. The validity of these calculations have been verified by Becker *et al.* [53,54] in their photoelectron studies of the decay of valence satellite states in neon and argon. In our autoionization studies of doubly excited neutral Ne [55] we observed similar autoionizing transitions from $Ne^{**}(2s^2 2p^4)^1D 3pn\ell \rightarrow Ne^{+}*(2s^2 2p^4)^3P 3p + e$. In addition, we have observed radiative decay (in the vacuum UV region) from the $Ar^{+}(3s^2 3p^4)^1Dnd$ states for $n=3,4$, and 5. However, above $n=5$ the fluorescence suddenly stops [56]. Because the energy of the $n=6$ level lies above or coincides with the ^3P double ionization threshold [57–60] it is reasonable to assume that the sudden disappearance of fluorescence above $n=5$ implies that the nonradiative pathway of autoionization is the more probable one for $n \geq 6$.

Electron recapture by the Ar^{2+} states given by Eqs. (2) and (3) create the states

$$Ar^{+}(3s^2 3p^4)^1D,{}^1Sn\ell, \tag{6}$$

$$Ar^{+}(3s3p^5)^3P,{}^1Pn\ell, \tag{7}$$

and the ^3P state given by Eq. (5). These are precisely the states discussed above. The decay pathway for the $(3s^0 3p^6)^1Sn\ell$ state [Eq. (4) plus electron recapture] is unknown but we would expect autoionization to be the dominant pathway because its lowest level is well above the double-ionization threshold. However, as we will see, the population of the initial $Ar^{2+}(3s^0 3p^6)^1S$ is only a few percent of all final states produced by the ejection of a $2p$ electron.

The percent distribution for producing the Ar^{2+} final states in Eqs. (2)–(4) can be determined from the measurements of the relative intensities of the lines in the $L_{2,3}$MM Auger electron spectrum. These measurements have been made by Mehlhorn [49] and by Werme, Bergmark, and Siegbahn [50]. We have listed their percent distributions for both the $L_3\,MM$ and $L_2\,MM$ transitions in Table II. We see that both sets of data are in substantial agreement with each other. Measurements by Carlson and Krause [61] did not resolve the $(3s^2 3p^4)^3P,{}^1D$, and ^1S transitions. However, they quote an integrated intensity of 76% of the total, in

TABLE II. Percent population of the Ar $L_{2,3}$ MM Auger decay channels.

Ar^{2+} final state		L_3 vacancy		L_2 vacancy	
		Ref. [50]	Ref. [49]	Ref. [50]	Ref. [49]
$(3s^2 3p^4)$	^3P	33.4	33.1	29.9	30.7
	^{1}D	33.1	36.4	39.4	37.3
	^1S	12.3	9.7	12.0	9.6
$(3s3p^5)$	^3P	10.6	8.8	8.0	10.3
	^{1}P	6.5	6.3	6.8	6.5
$(3s^0 3p^6)$	^{1}S	4.2	5.7	3.9	5.5

good agreement with the above authors. The calculations by McGuire [62] are in accord with the experimental results.

From Table II we see that about 33% of the final states formed are in the $(3s^2 3p^4)^3P$ states. After electron recapture by this state only radiative decay can occur. According to the calculations of Armen and Larkins [51,52] the remaining states should decay only by autoionization, provided the appropriate n values lie above the double-ionization threshold. We do not know what n values will be populated in the recapture process. However, on the basis of our branching ratio results, that the Ar^+ yield is about 33% of the total ion yield at the L_3 edge, we conclude that electron recapture into the remaining Ar^{2+} ions must populate sufficiently high n values to allow subsequent autoionization into Ar^{2+}. Typically, this requires $n \geqslant 6$ for the $(3s^2 3p^4)^1D, {}^1Sn\ell$ states. Autoionization from these levels should produce a discrete low-energy electron spectrum that is independent of the incident photon energy. For example, autoionization of $Ar^+(^1D)6d, 7d$, and $8d$ levels into Ar^{2+} (^3P) will produce electrons with energies of 0, 0.5, and 0.8 eV, respectively. Decay of the $(^1S)5d$ state should produce 1.3 eV electrons. We have taken the binding energies of the $(^1D)nd$ states form Ref. [57] and that of the $(^1S)5d$ level from Ref. [63]. Such studies will be necessary to determine the n values that are populated in the recapture process.

D. Fluorescence induced by electron recapture

Detailed measurements of the fluorescence produced by radiative decay of the $Ar^+(3s^2 3p^4)^3Pnd$ states provides another important technique to study the dynamics of electron recapture and the shake-up processes that are predicted to occur in the formation of the discrete Rydberg series leading to the L_3 and L_2 edges. Most of this radiation occurs between 200 and 600 nm and in the vacuum UV between 55 and 80 nm [56]. We have observed the undispersed fluorescence with a bandpass of 300 to 550 nm [64]. This spectrum is compared to the Ar^+ ion yield in Fig. 7. The fluorescent spectrum is superimposed on a large continuum of scattered radiation and the dashed line indicates an approximate base line. We can see a very close agreement between the two curves including the PCI induced decay of the Ar^+ continuum above the L_2 edge. Rühl, Heinzel, and Jochims [65] have also observed fluorescent radiation in this region and the PCI induced decay. This is clear evidence that electron recapture has occurred. In addition, fluorescence is observed from the $2p^{-1}(3s^2 3p^6)4s$ absorption line at 5.07 nm (244.39 eV). However, if the $4s$ electron remains a spectator during Auger decay the final state would be $(3s^2 3p^4)^3P4s$, which can decay only by emitting 72 to 73 nm radiation. This emission would not be observed in our fluorescent spectrum. However, shake-up into the $5s$ level during the Auger decay would produce visible radiation from the $5s \rightarrow 4p$ and $4p \rightarrow 4s$ transition (413-497 nm), which would be observed. Note that shake-up into the $3d$ level can produce only radiation in the vacuum UV and would not be observed in our spectrum. Thus observation of fluorescence at the $2p$–$4s$ transition energy provides evidence of shake up from the $4s$ to the $5s$ level during Auger decay of the $2p$ hole. This particular shake-up and many others have been observed by Aksela *et al.* [66] using the technique of resonance Auger-electron spectrometer.

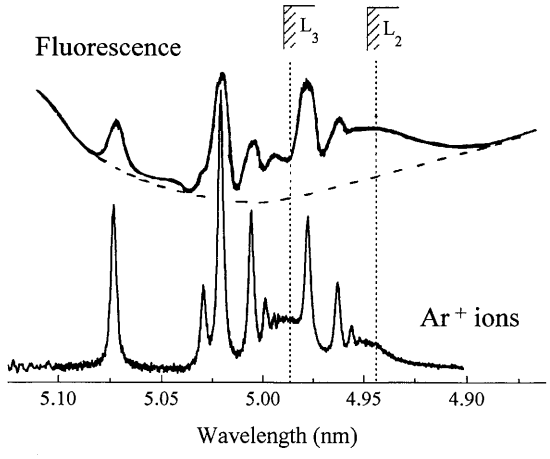

FIG. 7. Undispersed fluorescence (300–550 nm) from Ar excited by synchrotron radiation between 5.1 and 4.9 nm (243–253 eV). The dashed line indicates the approximate base line above a scattered light continuum. The Ar^+ spectrum from Fig. 1 is shown for comparison.

The one notable difference between the Ar^+ yield and the fluorescent yield is that the nominal $5d$ lines at 5.0 nm and 4.96 nm appear to be missing in the fluorescent signal! This may be caused by shake-up into the $(^1D)6d, 7d$ and $(^1S)6d$, $7d$ levels [63,67] which autoionize leaving only the $(^3P)6d, 7d$ lines to fluorescence. Or, possibly fluorescence from this level occurs in the vacuum UV and would not be detected in our studies. Clearly, higher resolution is desirable when studying the undispersed fluorescent spectrum (see Fig. 7). Studying the dispersed fluorescence at all wavelengths should prove to be a valuable additional technique to help in our understanding of the Auger decay process.

E. Line-width measurements

The $2p^{-1}(3s^2 3p^6)ns, n'd$ resonance lines observed in the Ar^+ and Ar^{2+} ion yield spectra show some interesting line width variations. Measurements of the half-widths of the Ar^+ lines are all about 120 meV. A high-resolution measurement (20 meV instrumental resolution) of the $2p^{-1}(3s^2 3p^6)4s$ line at 244.4 eV gave a value of 118 ± 4 meV. However, in the Ar^{2+} spectrum only the $4s$ and $3d$ lines below the L_3 edge have half-widths of 120 meV. The $4d$ line at 247.67 eV has a width of 140 meV and the nd series above the L edge have widths of 226 meV. These variations can be explained as follows:

Below the L_3 edge, when the initial state $2p^{-1}(3s^2 3p^6)4d$ decays, the most probable final states are $Ar^+(3s^2 3p^4)5d$ and $6d$, caused by shake-up of the $4d$ electron [63]. The $Ar^+(3s^2 3p^4)^3P5d$ and $6d$ states can decay only by fluorescence producing Ar^+, whereas the $(3s^2 3p^4)^1D, {}^1S6d$ states autoionize producing Ar^{2+} (see the discussion in Sec. III C). Because autoionization lifetimes are comparable to the Auger decay lifetime the $Ar^{2+}4d$ lines are broadened considerably. Above the L_3 edge, when the hole-state decays into $Ar^+(3s^2 3p^4)nd$, all the excited states

can autoionize into the L_3 continuum, producing Ar^{2+} and causing broadening of the observed lines. The above processes can explain the variation in line widths observed by King and Read [45]. In their study of the same resonances they used an electron-energy-loss technique, which is analogous to a total absorption spectrum. Below the L_3 edge they obtained a half-width of 116 ± 3, 118 ± 4, and 142 ± 14 meV for the $4s,3d$, and $4d$ lines, respectively. Above the L_3 edge they obtained 132 ± 10 meV for the nd series. If we take the sum of our ion yield spectra we obtain a total ion yield curve which is similar to that published by King and Read. The degree of broadening of an individual line in a total absorption spectrum depends upon the width and relative intensity of the line in the partial ion yield spectra.

ACKNOWLEDGMENTS

The authors are grateful to Professors M. Ya. Amusia and F. P. Larkins for valuable discussions and for pointing out the possibility that autoionization of excited ionic states produced by electron recapture could account for the anomalous Ar^{2+} signals observed. We also wish to thank Professors W. Mehlhorn and T. Åberg for their numerous and invaluable discussions, which helped to guide our thoughts in the analysis of our results. It is with pleasure that we acknowledge the help of Professor D. Lindle, Dr. P. Glans, Dr. H. H. Wang, and Dr. J. Bozek. We are particularly indebted to Dr. J. Underwood for time on the 6.3.2 beamline and the use of his facilities. This research was supported by the National Science Foundation under Grant No. PHY-9410716 and performed at the Advanced Light Source, Berkeley, CA.

[1] R. B. Barker and H. W. Berry, Phys. Rev. **151**, 14 (1966).
[2] P. J. Hicks, S. Cvejanović, J. Comer, F. H. Read, and J. M. Sharp, Vacuum **24**, 573 (1974).
[3] H. G. Heideman, G. Nienhuis, and T. van Ittersum, J. Phys. B **7**, L493 (1974).
[4] A. J. Smith, P. J. Hicks, F. H. Read, S. Cvejanović, G. C. King, J. Comer, and J. M. Sharp, J. Phys. B **7**, L496 (1974).
[5] G. Nienhuis and H. G. M. Heidemann, J. Phys. B **8**, 2225 (1975).
[6] F. H. Read, Radiat. Res. **64**, 23 (1975).
[7] M. J. Van der Wiel, G. R. Wight, and R. R. Tol, J. Phys. B **9**, L5 (1976).
[8] V. Schmidt, N. Sander, and W. Mehlhorn, Phys. Rev. Lett. **38**, 63 (1977).
[9] V. Schmidt, S. Krummacher, F. Wuilleumier, and P. Dhez, Phys. Rev. A **24**, 1803 (1981).
[10] Hanashiro, Y. Suzuki, T. Sasaki, A. Mikuni, T. Takayanagi, K. Wakiya, H. Suzuki, A. Danjo, T. Hino, and S. Ohtani, J. Phys. B **12**, L775 (1979).
[11] V. Schmidt, in *X-Ray and Atomic Inner-Shell Physics*, edited by B. Crasemann AIP Conf. Proc. No. 94 (AIP, New York, 1982), p. 544.
[12] R. Hustler and W. Mehlhorn, Z. Phys. **307**, 67 (1982).
[13] S. H. Southworth, U. Becker, C. M. Truesdale, P. H. Kobrin, D. W. Lindle, S. Owaki, and D. A. Shirley, Phys. Rev. A **28**, 261 (1983).
[14] W. Mehlhorn, in *Physics of Atoms and Molecules*, edited by B. Crasemann (Plenum Press, New York, 1985), p. 119.
[15] T. Hayaishi, Y. Morioka, Y. Kageyama, M. Watanabe, I. H. Suzuki, A. Mikuni, G. Isoyama, S. Asaoka, and M. Nakamura, J. Phys. B **17**, 3511 (1984).
[16] M. Borst and V. Schmidt, Phys. Rev. A **33**, 4456 (1986).
[17] P. A. Heimann, D. W. Lindle, T. A. Ferrett, S. H. Liu, L. J. Medhurst, M. N. Piancastelli, D. A. Shirley, U. Becker, H. G. Kerkhoff, B. Langer, D. Szostak, and R. Wehlitz, J. Phys. B **20**, 5005 (1987).
[18] T. Hayaishi, E. Murakami, A. Yagishita, F. Koike, Y. Morioka, and J. E. Hansen, J. Phys. B **21**, 3203 (1988).
[19] L. Avaldi, G. Dawber, R. Camilloni, G. C. King, M. Roper, M. R. F. Siggel, G. Stefani, and M. Zitnik, J. Phys. B **27**, 3953 (1994).
[20] L. Avaldi, R. I. Hall, G. Dawber, P. M. Rutter, and G. C. King, J. Phys. B **24**, 427 (1991).
[21] W. Eberhardt, S. Bernstorff, H. W. Jochims, S. B. Whitfield, and B. Crasemann, Phys. Rev. A **38**, 3808 (1988).
[22] K. Ueda, E. Shigemasa, Y. Sato, A. Yagishita, M. Ukai, H. Maezawa, T. Hayaishi, and T. Sasaki, J. Phys. B **24**, 605 (1991).
[23] N. Saito and I. H. Suzuki, Int. J. Mass Spectrom. Ion Processes **115**, 157 (1992).
[24] J. A. de Gouw, J. van Eck, J. van der Weg, and H. G. M. Heideman, J. Phys. B **25**, 2007 (1992).
[25] J. A. de Gouw, J. van Eck, J. van der Weg, and H. G. M. Heideman, J. Phys. B **28**, 1761 (1995).
[26] D. Čubrić A. A. Wills, J. Comer, and M. A. MacDonald, J. Phys. B **25**, 5069 (1992).
[27] D. Čubrić, A. A. Wills, E. Sokell, J. Comer, and M. A. MacDonald, J. Phys. B **26**, 4425 (1993).
[28] G. C. King, F. H. Read, and R. C. Bradford, J. Phys. B **8**, 2210 (1975).
[29] M. Ya. Amusia, M. Yu Kuchiev, S. A. Sheinerman, and S. I. Scheftel, J. Phys. B **10**, L535 (1977).
[30] M. Ya. Amusia, M. Yu. Kuchiev, and S. A. Sheinerman, Zh. Éksp. Teor. Fiz. **76**, 470 (1979) [Sov. Phys. JETP **49**, 238 (1979)].
[31] A. Niehaus, J. Phys. B **10**, 1845 (1977).
[32] A. Russek and W. Mehlhorn, J. Phys. B **19**, 911 (1986).
[33] P. van der Straten, R. Morgenstern, and A. Niehaus, Z. Phys. D **8**, 35 (1988).
[34] J. Tulkki, G. B. Armen, T. Åberg, B. Crasemann, and M. H. Chen, Z. Phys. D **5**, 241 (1987).
[35] J. Tulkki, T. Åberg, S. B. Whitfield, and B. Crasemann, Phys. Rev. A **41**, 181 (1990).
[36] G. B. Armen, S. L. Sorensen, S. B. Whitfield, G. E. Ice, J. C. Levin, G. S. Brown, and B. Crasemann, Phys. Rev. A **35**, 3966 (1987).
[37] G. B. Armen, J. Tulkki, T. Åberg, and B. Crasemann, Phys. Rev. A **36**, 5606 (1987).
[38] G. B. Armen, Phys. Rev. A **37**, 995 (1988).
[39] G. B. Armen, J. C. Levin, and I. A. Sellin, Phys. Rev. A **53**, 772 (1996).

[40] R. W. Fink, R. C. Jopson, H. Mark, and C. D. Swift, Rev. Mod. Phys. **38**, 513 (1966).
[41] F. W. Saris and D. Onderdelinden, Physica **49**, 441 (1970).
[42] J. A. R. Samson, J. N. Cutler, Z. X. He, W. C. Stolte, and J. D. Bozek, Bull. Am. Phys. Soc. **40**, 1286 (1995).
[43] J. A. R. Samson, Z. X. He, W. C. Stolte, and J. N. Cutler, J. Electron Spectrosc. Relat. Phenom. **78**, 19 (1996).
[44] J. A. R. Samson, Z. X. He, R. Moberg, W. C. Stolte, and J. N. Cutler, Can. J. Phys. (to be published).
[45] G. C. King and F. H. Read, in *Physics of Atom and Molecules*, edited by B. Crasemann (Plenum Press, New York, 1985), p. 317.
[46] W. S. Watson, J. Phys. B **5**, 2292 (1972).
[47] D. R. Denne, J. Phys. D **3**, 1392 (1970).
[48] E. Gilberg, M. J. Hanus, and B. Foltz, Rev. Sci. Instrum. **52**, 662 (1981).
[49] W. Melhorn, Z. Phys. **160**, 247 (1968).
[50] L. O. Werme, T. Bergmark, and K. Siegbahn, Phys. Scr. **8**, 149 (1973).
[51] G. B. Armen and F. P. Larkins, J. Phys. B **24**, 741 (1991).
[52] G. B. Armen and F. P. Larkins, J. Phys. B **25**, 931 (1992).
[53] U. Becker, R. Wehlitz, O. Hemmers, B. Langer, and A. Menzel, Phys. Rev. Lett. **63**, 1054 (1989).
[54] U. Becker, O. Hemmers, B. Langer, I. Lee, A. Menzel, R. Wehlitz, and M. Ya. Amusia, Phys. Rev. A **47**, R767 (1993).
[55] J. A. R. Samson, Y. Chung, and E. M. Lee, Phys. Rev. A **45**, 259 (1992).
[56] J. A. R. Samson, Y. Chung, and E. M. Lee, Phys. Lett. A **127**, 171 (1988).
[57] M. O. Krause, S. B. Whitfield, C. D. Caldwell, J.-Z. Wu, P. van der Meulen, C. A. de Lange, and R. W. C. Hansen, J. Electron Spectrosc. Rel. Phenom. **58**, 79 (1992).
[58] C. E. Brion and A. O. Bawagan, Chem. Phys. Lett. **134**, 76 (1987).
[59] V. Schmidt, Z. Phys. D **2**, 275 (1986).
[60] H. Kossmann, B. Krassig, V. Schmidt, and J. E. Hansen, Phys. Rev. Lett. **58**, 1620 (1987).
[61] T. A. Carlson and M. O. Krause, Phys. Rev. Lett. **17**, 1079 (1966).
[62] E. J. McGuire, Phys. Rev. A **11**, 1880 (1975).
[63] M. Meyer, E. v. Raven, B. Sonntag, and J. E. Hansen, Phys. Rev. A **43**, 177 (1991).
[64] J. A. R. Samson, E. M. Lee, and Y. Chung (unpublished data).
[65] E. Rühl, C. Heinzel, and H. W. Jochims, Chem. Phys. Lett. **211**, 403 (1993).
[66] H. Aksela, S. Aksela, H. Pulkkinen, G. M. Bancroft, and K. H. Tan, Phys. Rev. A **37**, 1798 (1988).
[67] M. Meyer, E. V. Raven, B. Sonntag, and J. E. Hansen, Phys. Rev. A **49**, 3685 (1994).